第20回性能に基づく橋梁等の耐震設計に関する
シンポジウム講演論文集（2017年7月）

Study about the Relationship between Applied Pressure on Bridge and the Hydrostatic Pressure

Chunyan XING[1], Kenji KOSA[2] and Takashi SATO[3]

[1] Graduate Student, Dept. of Civil Engineering, Kyushu Institute of Technology
(〒804-8550, Sensui 1-1,Tobata, Kitakyushu, Japan)
[2] Ph.D., Professor, Dept. of Civil Engineering, Kyushu Institute of Technology
(〒804-8550, Sensui 1-1,Tobata, Kitakyushu, Japan)
[3] Engineer, Structural Engineering Division, Chodai Co., Ltd.

1. INTRODUCTION

Not only coastal structures but many infrastructures, bridges and buildings, which located inland, were also damaged by the tsunami due to the Great East Japan Earthquake in 2011[1)]. The damage of bridge girders caused loss of valuable social capital and delayed to rescue people and supply goods. After the tsunami damage, the authors carried out a reconnaissance visit to the coast of Tohoku region and observed that many bridge girders in Tohoku region were washed away by the tsunami[2)]. So that it was significant to know how to evaluate tsunami force applied on bridge girder and propose a design method of tsunami force on bridge girder.

In previous research[3)], a series of tsunami experiments have been carried out. The horizontal force applied on a girder has been evaluated based on the girder position parameter case. As a consequence, pressure on the leading edge of girder model increases linearly with girder position decreasing.

This research uses CADMAS-SURF/3D, a computational dynamics software, to simulate the previous solitary wave experiments. The mechanism of the horizontal pressure acting on the leading edge of girder changing with different girder positions is discussed.

2. HYDRAULIC EXPERIMENT

This section introduces the apparatus and experimental results of hydraulic experiments.

As illustrated in Fig. 1, a 41 m long, 0.8 m wide, 0.95 m high open channel is used for the hydraulic experiments. A solitary wave is generated by a wave making plate, and then spreads to girder model. Six wave gauges and two propeller velocity meters are set up along the open channel. Both H6 and V1 are set the medium of girder to measure the wave height and velocity applying on girder model. The prototype of bridge girder model is a damaged bridge at Sumatra land of Indonesia, due to India Ocean Tsunami. As shown in Fig. 2, the scale of this bridge model is 1/50. Its length, width and height were made to 400 mm, 190 mm and 34 mm (prototype: 19.1m-long, 10.2m-wide and 1.7m-high), respectively. The width of model prototype has a similar scale to some of the national road bridges in Japan such as Utatsu bridge(14.4m-long, 0.8m-wide and 1.2m-high). For the hydraulic experiment, 20 pressure gauges were set around the girder to measure the horizontal pressure on girder. In particular, pressure gauge P3, which was set the center of the leading edge of girder, will be used as an example to discuss the relationship between the horizontal pressure and girder position.

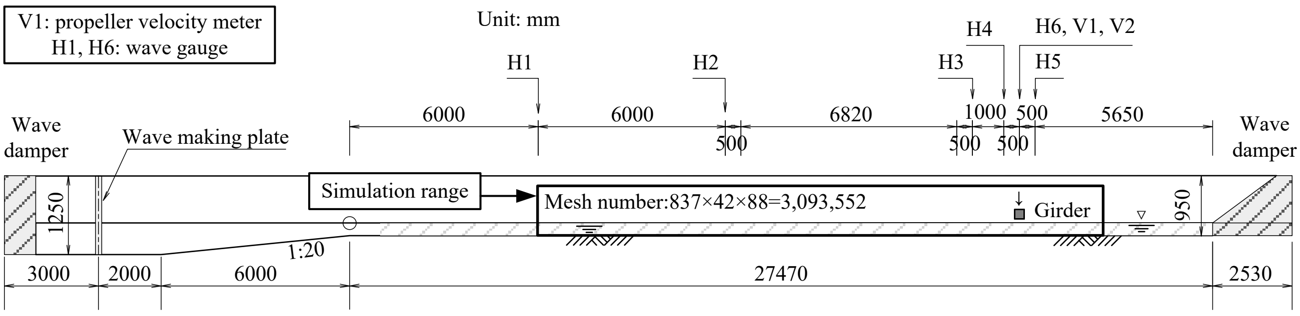

Fig. 1 Experimental apparatus

Fig. 3 shows the experimental cases. In this paper, the research focuses on a solitary wave, which is used for simulating the front part of tsunami wave. All 3 experimental cases in Fig. 3 have the same water level (35cm) and the same wave height (20cm). The experimental parameter is girder position Z, which shows the height between the initial water surface and the bottom of girder model.

Experimental result of those 3 cases is denoted in Fig. 4. Horizontal axis shows pressure. Vertical axis shows girder position Z/a_H (For case 3: Z/a_H=16.6cm/20cm=0.83≈0.8). The triangle mark shows the pressure applying on the leading edge of girder. The chain line shows the pressure line with zero value. The triangle mark shows the pressure acting on the leading edge of girder. The pressures acting on the leading edge of girder of Z/a_H=0, 0.4 and 0.8 are 1942 Pa, 1304 Pa and 991 Pa, respectively. This pressure increases linearly with the girder position decreasing. The hydrostatic pressure, which is calculated by the inundation height of H6, is denoted by the dot mark and the dotted line. For Z/a_H=0 case, the hydrostatic pressure is 1896 Pa, which is almost same with the pressure acting on the leading edge of girder. Whereas, for other two cases, the hydrostatic pressure are smaller than the pressure acting on the leading edge of girder. The difference between hydrostatic pressure and pressure acting on leading edge of girder of Z/a_H =0.4 case is bigger than that of Z/a_H =0.8 case. Therefore, the discussion of the Z/a_H =0.4 case, which has the middle girder height, has been eliminated. The simulation analysis of Z/a_H =0 and 0.8 case are carried out to know mechanism of the pressure acting on the leading edge of girder changing with different girder positions.

3. SIMULATIVE CONDITIONS

This section introduces the simulative conditions of this paper.

A 3-dimensional open channel model and a 3-dimensional girder model are used. The simulative girder model has shown in Fig. 5. The girder model has 400mm-long, 190mm-wide and 34mm-high, which is totally same experimental girder model. The side view of girder model has shown in Fig. 5-(a). At X direction, the 190mm-long girder is divided to 37 meshes. Mesh size of every inner girder is 6mm, and 5mm for others. At Z direction, the 34mm-high girder is divided to 6 meshes. Mesh size on top of girder is 4mm, and 5mm for others. The front view of girder model has shown in Fig. 5-(b). At Y direction, the 400mm-long girder is divided to 20 meshes. Mesh size of every inner girder is 20mm. In addition, the position of pressure gauge P3 has denoted by red cell in the same figure. The horizontal pressure is measured by the cells front of girder cells. The mesh division of this simulation analysis has illustrated in Fig. 6. As shown in Fig. 6-(a), the simulative field starts from wave gauge H1, ends between girder model and the wave damper. The number of all meshes is 3,093,552 [= 837 (length direction) × 42 (width direction) × 88 (height direction)]. The open

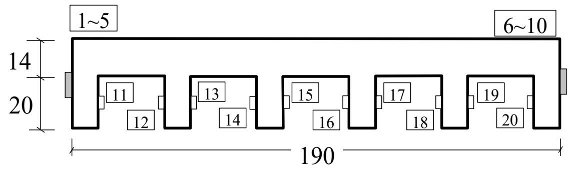

(a) Side view

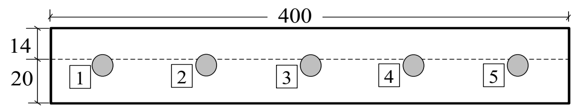

(b) Front view

Fig. 2 Girder shape and position of pressure gauges

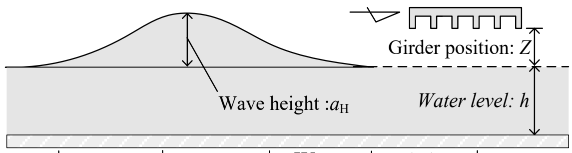

Case	Wave shape	Water level h [cm]	Wave height a_H [cm]	Girder position Z [cm]	Z/a_H
1	Solitory	35	20	0	0
2				8.3	0.4
3				16.6	0.8

Fig. 3 Experimental cases

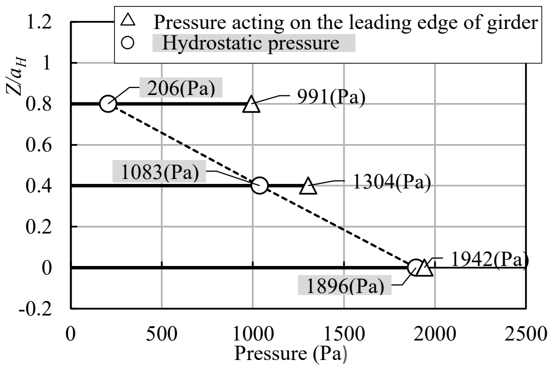

Fig. 4 Experimental result

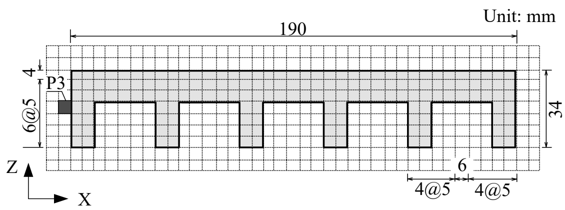

(a) Side view

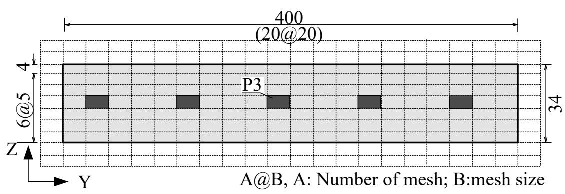

(b) Front view

Fig. 5 Simulative girder shape and position of P3

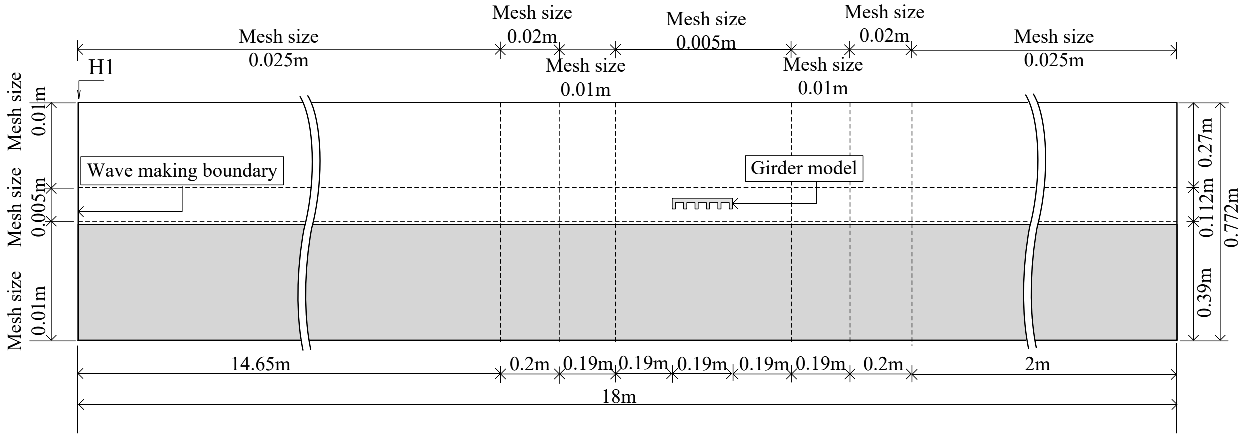

(a) Side view

channel model has 18m long, 0.80 m wide and 0.772m high. At the length direction, mesh size is 0.005m near the girder, and then it is enlarged to be 0.025m near the inlet and outlet boundary. As shown Fig.6-(b), the mesh is 0.02m at the width direction. There are 0.01m interspace between girder model and side wells, where wave can go through totally.

The simulative conditions are introduced as below: Input data of wave making model included both wave height data and velocity data. We attempted to explain the input method in detail.

Because the simulation model starts from H1, the experimental wave height of H1 is set as the wave height data in this simulation analysis.

Input velocity data is considered as below: Since there is no experimental velocity data in the hydraulic experiment at H1, the input velocity is computed by Eq. (1) based on the Boussinesq's theory[5]:

$$u_x = \sqrt{\frac{g}{h}}\eta\{1-\frac{\eta}{4h}+[h^2-\frac{3}{2}(h+z)^2](\frac{a_H}{h^3}-\frac{3\eta}{2h^2})\} \qquad \text{Eq. (1)}$$

Here, u_x is the horizontal velocity of water particles at point z; z represents the height from the water bottom to the calculated point and η is the change of water level.

The numerical condition of this simulation are introduced as below: Based on CADMAS Manual[6], the numerical model is ran by Reynolds Averaged Navier Stokes simulations. Volume of fluid (VOF) method is used to simulation the wave surface of experiment. The bottom of water channel is set to be slip, where the pressure and velocity are calculated by the same way at inner of open channel. In addition, only small amplitude wave can completely get through the back of open channel.

4. NUMERICAL RESULTS OF Z/a_H=0 CASE

In this section, simulative results of Z/a_H=0 case of wave height, velocity and pressure are discussed by comparison between the calculated results and experimental results. In addition, authors try to explain the mechanism of horizontal pressure changing with different

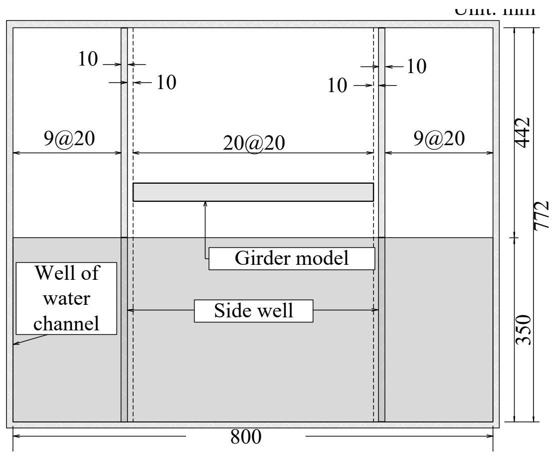

(b) Front view

Fig. 6 Mesh division of this simulation analysis

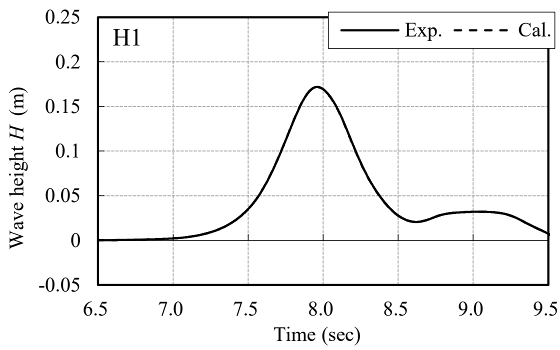

Fig. 7 Wave height time history of H1

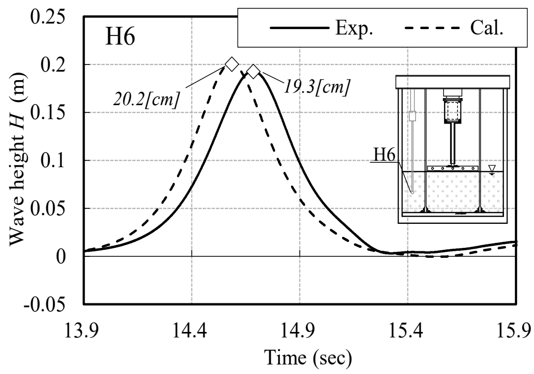

Fig. 8 Wave height time history of H6

girder position cases.

(1) Comparison between calculated results and experimental results

Firstly, the wave height at wave making boundary was checked. Fig. 7 shows the wave height history at H1 (wave making boundary). The full line was experimental result and the dotted line was calculated results. We noted that the calculated wave completely coincided with experimental wave at H1. Figure 8 shows the wave height time history at H6, which is set beside of the girder. The full line shows the experimental result and the broken line shows the calculated results. The time history shape of experimental data and calculated data are almost same. The peak wave height of experiment and calculation is 19.3 cm and 20.2 cm. Because their peak difference is small, it is reasonable to say good agreement is observed between the calculated and experimental wave height.

Next, V1 is selected as an example to check the velocity reproduction and the time history is plotted in Fig. 9. V1 is a propeller velocity meter, which locates in the center of girder. The calculated peak agrees well with hydraulic experimental peak.

And then, P3 is selected as an example to check the pressure reproduction and the time history is denoted in Fig. 10. Because the experimental pressures of P1~P5 are almost same[7], the pressure gauge P3, which is set in front center of girder model, is taken as a representative to discuss the pressure reproduction of this simulation analysis. The measured pressure cell of P3 has illustrated in Fig. 5. In Fig. 10, the full line shows the experimental result and the broken line shows the calculated results. The experimental pressure peak is 1942 Pa. The calculated peak is 1740 Pa, which can reappear 90% of experimental peak.

Finally, the wave shape reproduction of this simulation is checked. As shown in Fig. 10, at 14.3 sec (time [a]), the solitary wave is acting on girder and pressure of P3 is increasing. When it goes to be 14.5 sec (time [b]), pressure of P3 reaches its peak. The wave shape time [a] and [b] are taken as examples to explain the reproduction of this simulation analysis. In addition, calculated pressure reaches its peak about 0.079sec later than the experimental one. Assuming P3.cal and P3.exp reach their peak at the same time, all experiment data is moved ahead by 0.079 sec. The comparison between experimental figure and simulative snapshots of time [a] and time [b] has shown in Fig. 11 and Fig. 12, respectively. The initial water surface is marked by chain line for all wave shape figures.

As shown in Fig. 11-(a), the wave surface is highlighted by the full line. Wave height front of girder H.exp is measured to be 87 mm. At the same time, the snapshot of simulation analysis is denoted in Fig. 11-(b). The full line and dotted line show the simulative wave surface and experimental wave surface, respectively. The calculated wave height front of girder H.cal is

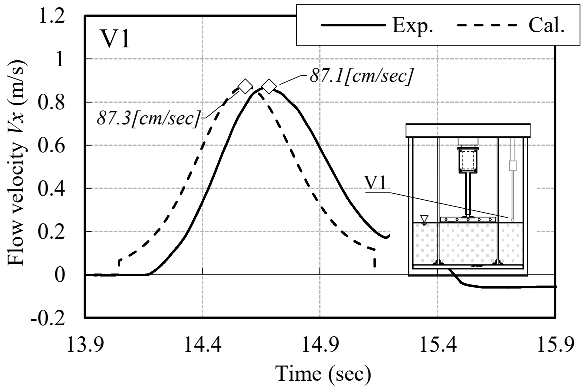

Fig. 9 Velocity time history of V1

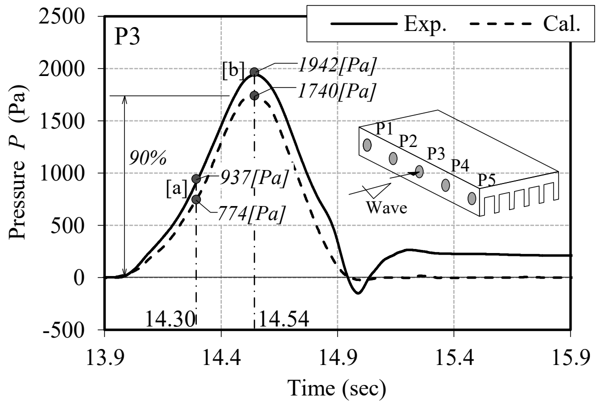

Fig. 10 Pressure time history of P3

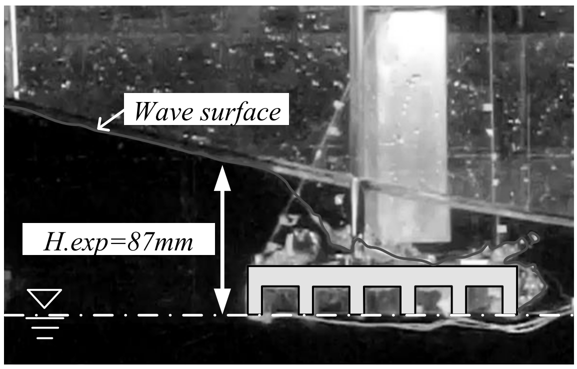

(a) Experiment

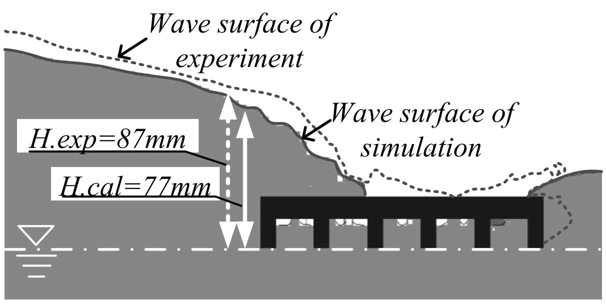

(b) Simulation

Fig. 11 Wave shape at [a] 14.30 sec

77mm, which is about 11 % (=87-77/87×100%) smaller than H.exp. Moreover, as shown in Fig. 10, P3.cal is 770 Pa at 14.30 sec, which is about 17% (=937-774/937 × 100%) smaller than P3.exp. Authors think the smaller calculated wave height leads the calculated pressure to be smaller than the experimental one. Furthermore, the simulative wave lags a little behind the experimental wave as shown in Fig. 11-(b).

Move to time [b], as shown in Fig. 12-(a), the wave surface is highlighted by the full line. And the wave height front of girder H.exp is measured to be 216 mm. At the same time, the snapshot of simulation analysis is denoted in Fig. 12-(b). The full line and dotted line show the simulative wave surface and experimental wave surface, respectively. The wave height H.cal is 213mm, which is about 1.4% (=216-213/216×100%) smaller than H.exp 207mm, which leads P3.cal to 10% (=1942-1740/1942× 100%) be smaller than P3.exp. Compare the simulative wave shape with the experimental one, it is noted that the simulative one lags a little behind the experimental wave.

(2) Comparison between calculated pressure and hydrostatic pressure

This subsection will discuss the relationship between calculated pressure and hydrostatic pressure. In CADMAS simulation analysis, pressure is calculated by N-S equations. And the pressure distribution at vertical direction is computed by Eq. (2) as below:

$$Z-\frac{1}{\rho}\frac{\partial p}{\partial z}=$$
$$\frac{\partial u_z}{\partial t}+u_x\frac{\partial u_x}{\partial x}+u_y\frac{\partial u_y}{\partial y}+u_z\frac{\partial u_z}{\partial z}-\upsilon(\frac{\partial^2 u_x}{\partial x^2}+\frac{\partial^2 u_y}{\partial y^2}+\frac{\partial^2 u_z}{\partial z^2})$$

Eq. (2)

Here, ρ: density of water; Z: acceleration of mass force, and Z=-g=-9.8 m/s^2; υ: coefficient of viscosity, which is set to be 10^{-6} in this simulation; u_x, u_y and u_z are the velocity of X, Y and Z direction. $\frac{\partial u_z}{\partial t}+u_x\frac{\partial u_x}{\partial x}+u_y\frac{\partial u_y}{\partial y}+u_z\frac{\partial u_z}{\partial z}$ shows inertia term, which includes variation term and convection term; $\upsilon(\frac{\partial^2 u_x}{\partial x^2}+\frac{\partial^2 u_y}{\partial y^2}+\frac{\partial^2 u_z}{\partial z^2})$ is diffusion term. In this paper, "S" is used to explain the acceleration from inertia term and diffusion term as following:

$$S=\frac{\partial u_z}{\partial t}+u_x\frac{\partial u_x}{\partial x}+u_y\frac{\partial u_y}{\partial y}+u_z\frac{\partial u_z}{\partial z}-\upsilon(\frac{\partial^2 u_x}{\partial x^2}+\frac{\partial^2 u_y}{\partial y^2}+\frac{\partial^2 u_z}{\partial z^2})$$

Eq. (2-1)

So that Eq. (2) changes to be Eq. (2-2) as below:

$$dp=(g+S)\rho dz \qquad \text{Eq. (2-2)}$$

When there are no wave, water velocity of every direction is going to be zero. Therefore, S equals 0. Substituting S=0

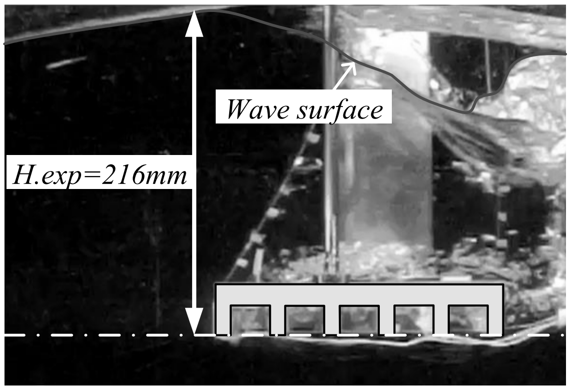

(a) Experiment

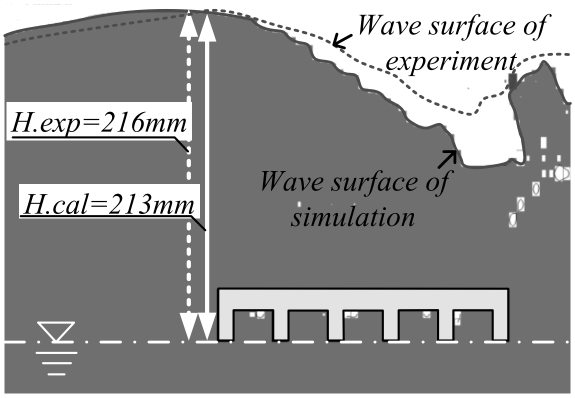

(b) Simulation

Fig. 12 Wave shape at [b] 14.54 sec

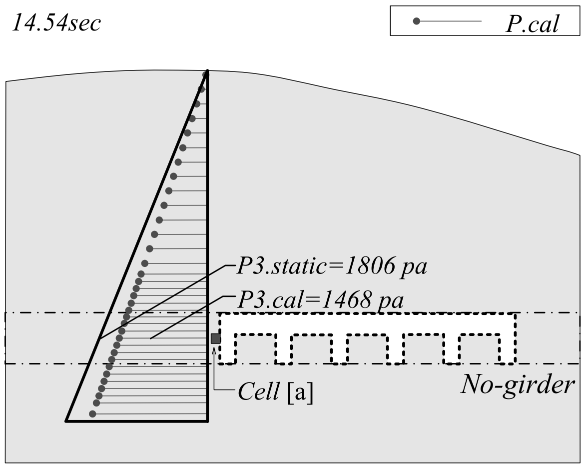

Fig. 13 Pressure distribution (No-girder case)

Table. 1 List of velocity terms of Cell [a] in Eq. (2-1)

Direction	Velocity (m/sec)		Variation term	Convection term	Diffusion term
	14.54sec	14.53sec			
X	0.872			-0.015	-2.960
Y	0.001			0.010	0.505
Z	0.004	0.026	-2.213	0.005	0.946

into Eq. (2), we obtain hydrostatic pressure formula Eq. (2-3) as below:

$$p = \rho g h \qquad \text{Eq. (2-3)}$$

Here, h: inundation height. N-S equation changes to be hydrostatic pressure equation.

In order to know the relationship between hydrostatic pressure and calculated pressure, pressure distribution of no-girder case is plotted in Fig. 13. As illustrated in the same figure, girder of Z/a_H=0 case locates the same position of the girder with broken line. The right triangle shows hydrostatic pressure, which is computed by Eq. (2-3). The calculated pressure of every mesh front of girder is plotted by the circle solid line, which is output from our simulation analysis directly. When wave reaches its peak at 14.54 sec, the pressure distribution shape of P.cal trends to be right triangle shape, which is similar with the pressure distribution shape of P.static. However, the calculated pressure of P3 is 1468 Pa, which is about 20% smaller than the hydrostatic pressure of P3. In other words, the triangle slope of P.cal is steeper than the triangle slope of hydrostatic pressure.

In order to know the reason of the steeper triangle pressure distribution of P.cal, authors try to use Eq. (2-1) and Eq. (2-2) to calculated P.cal of Cell [a] by hand, which has the same position of P3. All terms of Cell [a] in Eq. (2-1) are listed in Table.1. Because the variation term of X-direction and Y-direction are useless in Eq. (2-1), their data marked by slash is not used. Plug all of them into Eq. (2-1), S of Cell[a] can be computed to be -2 as below:

$$\begin{aligned} S &= -2.213 + [0.872 \times (-0.015) + (0.001) \times 0.010 + 0.004 \times 0.005] \\ &\quad - [10^{-6} \times (-2.960 + 0.505 + 0.946)] \\ &= -2 \end{aligned}$$

Using the same method, S of all cells from the wave surface to cell [a] almost equal to the same value of -2. Therefore, the hydrodynamic pressure distribution trends to be triangle shape. Moreover, the acceleration of mass of hydrodynamic is about 20% [= (9.8-2)/9.8] smaller than that of hydrostatic, which leads P3.cal to be about 20% smaller than P3.static.

As shown in Fig. 5, mesh size at Z-direction of P3 is 0.005m. Take S=-2 and dz=0.005m into Eq. (2-2), the pressure increment at cell [a] can be computed to 39 Pa as below:

$$dp = (9.8 - 2) \times 1000 \times 0.005 = 39(Pa)$$

As shown in Fig. 13, there are 24 meshes from the wave surface to Cell [a]. If we integrate all those 24 pressure increments, pressure of P3 is going to be 1324 Pa, which is similar with P3.cal 1468 Pa. So that using S value to compute P.cal is feasible.

As illustrated in Fig. 4, for Z/a_H =0 case the hydrostatic pressure is almost same with the pressure acting on the leading edge of girder. In order to know the relationship between hydrostatic pressure and calculated pressure of

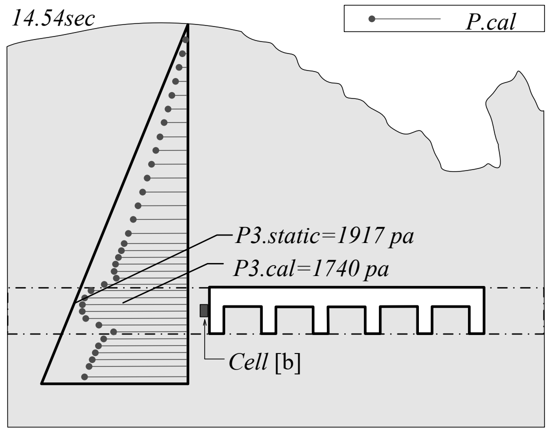

Fig. 14 Pressure distribution (with girder case)

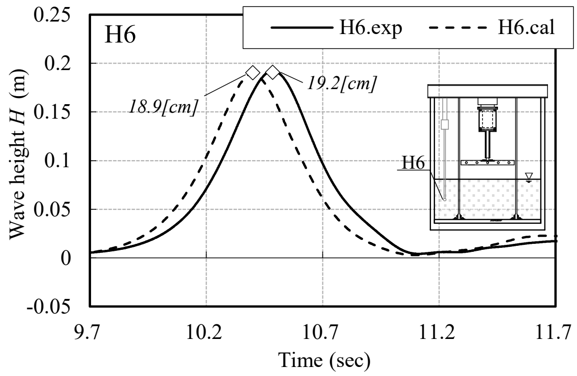

Fig. 15 Wave height time history of H6

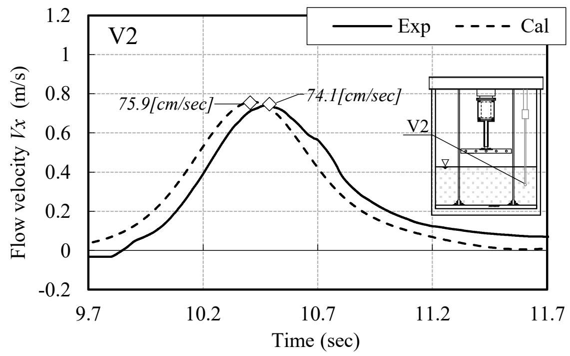

Fig. 16 Velocity time history of V2

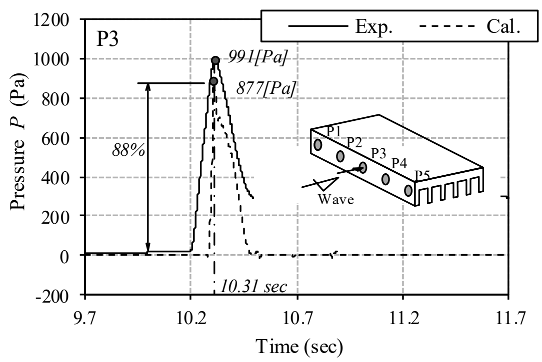

Fig. 17 Pressure time history of P3

Z/a_H =0 case with girder, pressure distribution at front of girder is plotted in Fig. 14. The pressure distribution shape of P.cal trends to be right triangle shape with a steeper slope than P.static, which is same with the hydrodynamic pressure distribution of on-girder case in Fig. 13. However, pressure increases sharply at the leading edge of girder and the value of P3.cal closes to that of P3.static. In order to know the sharply pressure change, authors try to calculate all pressure increments from the wave surface to Cell [b] by hand, which has the same position of P3. As a result, all 21 S values from wave surface to up of girder have a similar minus value of “-3”. But S values of the 4 cells at the leading edge of girder increases to be a big positive value about “+13” because the velocity increases at Z-direction. Pressure increment from the wave surface to cell [b] is calculated to be 2054 Pa. It is easy to understand that the closer girder the smaller velocity of X-direction becomes. And wave goes up along the leading edge of girder, which produces velocity of Z-direction increases sharply and the big positive value of S. Furthermore, P3.cal goes up to close P3.static.

5. NUMERICAL RESULTS OF Z/a_H=0.8 CASE

This section moves to the highest girder position case: Z/a_H=0.8 case.

The reproduction of wave height, velocity and pressure is explained in Fig. 15, 16 and 17, respectively. Fig. 15 shows the wave height time history at H6, which is set beside of girder. Both shape and peak of the experimental time history are same with the calculated one. Fig. 16 shows the velocity time history at V2, which is a propeller velocity meter inundated in the center depth of water. At the same figure, both shape and peak of the experimental time history are same with the calculated one. Therefore, good agreement both of wave height and velocity can be observed between experiment and simulation. P3 is selected as an example to check the pressure reproduction and the time history is plotted in Fig. 17. The full line shows the experimental result and the broken line shows the calculated results. The experimental pressure peak is 991 Pa. The calculated pressure reaches its peak 877Pa at 10.31 sec, which can reappear 88% of experimental peak.

The wave shape at 10.31 sec is taken as example to explain the reproduction of this simulation analysis. In addition, calculated pressure reaches its peak about 0.104 sec later than the experimental one. Assuming P3.cal and P3.exp reach their peak at the same time, all experiment data is moved ahead by 0.104 sec. The comparison between experimental figure and simulative snapshots of 10.31 sec has shown in Fig. 18. The initial water surface is marked by chain line for all wave shape figures. As illustrated in Fig. 18-(a), the wave surface is highlighted by the full line. And the wave height front of girder H.exp is measured to be 228mm. At the same time, the snapshot of simulation analysis is denoted in Fig. 18-(b). The full line and dotted line show the simulative wave surface and experimental wave surface, respectively. Here, H.cal and

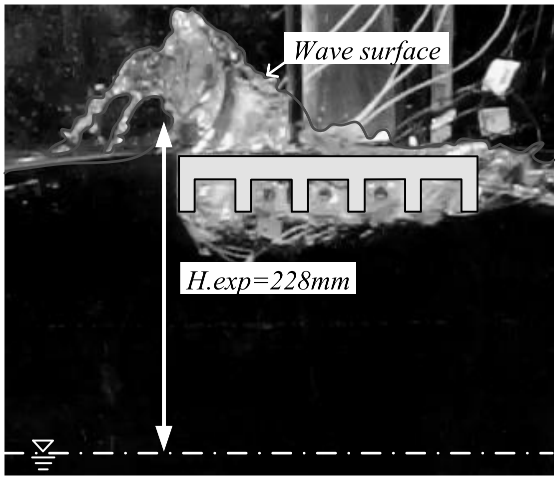

(a) Experiment

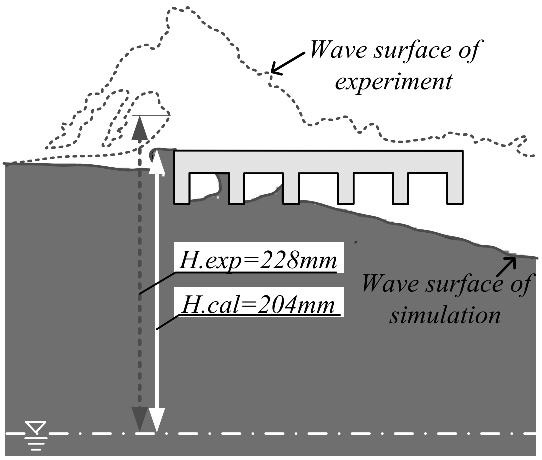

(b) Simulation

Fig. 18 Wave shape at 10.31 sec

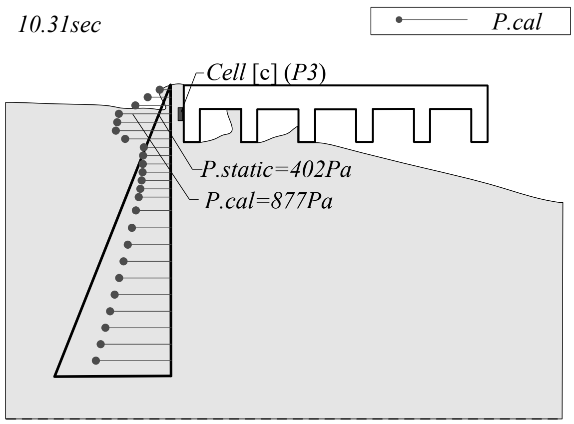

Fig. 19 Pressure distribution at 10.31 sec

Table. 2 Velocity list of Cell [c] in Fig. 19

Direction	Velocity (m/sec)		Variation term	Convection term	Diffusion term
	10.31sec	10.30sec			
X	0.308			-123.2	-24640
Y	-0.114			-0.3	-15
Z	0.795	0.946	-15.1	124.7	24931

H.exp indicate the wave height from the initial water level to wave surface of simulation analysis and experiment, respectively. H.cal is 204mm, which is about 11% (=228-204/228×100%) smaller than H.exp 228mm. The authors think the 12% pressure difference between P3.cal and P3.exp in Fig. 17 results from this 11% wave height difference.

The comparison between the calculated pressure and hydrostatic pressure is discussed as below: As illustrated in Fig. 4, for Z/a_H =0.8 case the hydrostatic pressure is smaller than pressure applying on the leading edge of girder. In order to know the pressure distribution on the leading edge of girder, the pressure distribution front of girder at 10.31sec is plotted in Fig. 19. Here, the right triangle shows hydrostatic pressure. The calculated pressure of every mesh is plotted by the circle solid line. The pressure distribution shape of P.cal also trends to be the triangle shape, which is similar with the shape of pressure distribution P.static. Cell [c] has the same position of P3. The inundation height of Cell [c] is 41 mm (=204mm+163mm). Plug it into Eq. (2-3), P.static equals to 402 Pa. So that P.cal is as twice (=877/402) much as P.static. To understand this high P.cal, pressure of cell[b] is calculated by hand. All terms of Cell [c] in Eq. (2-1) are listed in Table. 2. Because the variation term of X-direction and Y-direction are useless in Eq. (2-1), their data marked by slash is not used. Plug all of them into Eq. (2-1), S of Cell[c] can be computed to be 46 as below:

$$\begin{aligned} S &= -15.1 + [0.308 \times (-123.2) + (-0.114) \times (-0.3) + 0.795 \times 124.7] \\ &- [10^{-6} \times (-24640 - 15 + 24931)] \\ &= 46 \end{aligned}$$

As shown in Fig. 5, mesh size at Z-direction of P3 is 0.005m. Take S=46 and dz=0.005m into Eq. (2-1), the pressure increment can be computed to be 274 Pa as below:

$$dp = (46 + 9.8) \times 1000 \times 0.005 = 279(Pa)$$

As shown in Fig. 19, there are 4 meshes from the wave surface to Cell [c], and their pressure increments are 134 Pa, 224 Pa, 249 Pa, and the pressure of Cell [c] 274 Pa, respectively. If we integrate all those 4 pressure increments, pressure of P3 is going to be 881 Pa, which is similar with P3.cal 877 Pa. It is easy to understand that the closer girder the smaller velocity becomes. Moreover, because of the high girder position, S increases from the surface of wave, which produces P3.cal to be higher than P3.static.

6. CONCLUSIONS

Based on the pressure analysis on the leading edge of girder by experiment and CADMAS-SURF/3D simulation analysis, the conclusions can be summarized as below:

(1) For Z/a_H=0 of no-girder case, the pressure distribution shapes triangle, which is similar with the shape of hydrostatic pressure. In addition, because of the influence from velocity movement, S, the acceleration from inertia term and diffusion term in N-S equation, has a value about -2, which leads the hydrodynamic pressure to be about 20% smaller than its hydrostatic pressure.

(2)For Z/a_H=0 with girder case, the calculated pressure of P3 is 1942 Pa, which can reproduce the experimental pressure 1740 Pa well. When bottom of the solitary wave applied on the girder, S value from wave surface to up of girder has a similar minus value of "-3". But S at the leading edge of girder increases to be a big positive value about "+13" because of the velocity increase at Z-direction. Therefore, the calculated pressure of P3 1942 Pa is almost same with its hydrostatic pressure 1917 Pa.

(3)For Z/a_H =0.8 with girder case, the calculated pressure of P3 is 877 Pa, which can also reproduce the experimental pressure 991Pa well. When top of the solitary wave applied on the girder, S has a big positive value about +45 because the velocity increases at Z-direction at the leading edge of girder. Therefore, the calculated pressure 877 Pa is much higher than its hydrostatic pressure 402 Pa.

REFERENCES

1) Shimizu, H., Kosa, K., Sasaki, T. and Takeda, S. "Tsunami damage analysis in highway bridges", Journal of Structural Engineering, Vol. 58A, pp.366- 376, 2012. 3.
2) Rabbat, B.G. and Russel, H.G. "Friction coefficient of steel on concrete or grout", J. Structural. Eng., ASCE Vol. 111, No. 3, pp. 505-515, 1985.
3) Tanaka, M., Kosa, K., Sato, T. and Sasaki, T. "Tsunami damage analysis of concrete girder by girder position parameters", Proceedings of the JCI, Vol.38, No.2, pp. 829-834, 2016.
4) Nakagi, T., Kosa, K. and Sato, T. "Evaluation of properties of tsunami in the Kuji port", Coastal Engineering, Vol. 72, No. 2, p. I_1033-I_1038, 2016.
5) Library of Coastal Development Institute No.39 CADMAS-SURF/3D Research and Development of Numerical Open Channel, Coastal Development Institute of Technology, 2010.
6) Matsutomi, H, "Macroscopic analysis on a spilling breaker of solitary wave by using a bore model", Journal of JSCE, No. 387, pp. 263-272, 1987.
7) Hamai, S., Kosa, K., Sato, T., and Sasaki, T. "Experimental examination concerning the tsunami wave force to abutment", Journal of Structural Engineering, Vol. 62A, pp. 394-403, 2016.